

ASSESSING URBAN HEAT ISLAND IMPACT AND IDENTIFYING VULNERABILITY ZONES THROUGH GEOSPATIAL AND GEO-STATISTICAL TECHNIQUES

Debabrata NANDI¹, Debasish SING^{1,*}, Ashim BANIK¹, Partha Sarathi MISHRA²

¹ Department of Remote Sensing and GIS, MSCB University, Baripada, Mayurbhanj, Odisha, India, 757003

² Department of Computer sciences, MSCB University Takatpur, Baripada, Mayurbhanj, Odisha, India 757003

Abstract

An urban heat island emerged due to micro urban temperature variations are also referred to as urban heat islands or urban hot spots. The high-rise buildings along the roads form "Urban Canyons" that inhibit reflected radiation from the built-up surface. Urban heat island develops over the cities due to man-made activity and the landscape. An understanding of the urban heat island and its formation is not only helpful in understanding urban thermal characteristics but also helps in understanding human comfort. A geospatial technique has the ability to acquire updated and cost-effective data over large regions. For urban climatology studies, remote sensing and geographic information systems are an important source of information and an effective methodology. Since 1971, the city of Krishnanagar and its vicinity have been witnessing rapid urban growth. Due to its dense population, urban climate and rapid urban expansion, they cause environmental degradation. Appraisal and Impact of urbanization on micro-climate in the Krishnanagar city complex based on satellite derived parameters. For the years 1995, 2007 and 2018, several satellite image analysis approaches such as NDVI, NDWI and NDBI were computed. Significant differences in land surface temperature were observed between 1995 and 2007, as compared to 2007 and 2018.

Keywords: LULC; NDVI; NDWI; NDBI; Urban Heat Island (UHI); Linear Regression

Introduction

Urbanization is accelerating, leading to the rapid expansion of cities. In developing countries, the demand for built-up land frequently leads to the conversion of vegetated areas into urbanized land [1, 2]. This Unplanned urbanization and the resulting "Urban Heat Islands" (UHI) can have significant effect on rates of precipitation [3], human comfort, environment as well as terrestrial ecosystem [4-6]. Urban Heat Island (UHI) contributes to climate change in cities and surrounding areas [7-9], as well as the greenhouse effect and the breakdown of the environmental cycles [10-12].

The urban heat island (UHI) phenomenon effects negative impact due to fast and rapid urbanisation [13-15]. Because of the loss of vegetation, it is a result of cumulative land surface temperature (LST). LST play a vital role of surface-atmosphere interactions; it's played a crucial role in modelling hydrological, ecological, agricultural & meteorological processes on Earth surface [16-18]. Anthropologic factors, through changing land use and other activities, are the fundamental cause of environmental change on the earth [19-21].

Urban sprawl and the resultant Urban Heat Islands (UHI) can have directly affected the reflectivity or albedo of incoming solar radiation and emissivity [22, 23]. Urban heat island

* Corresponding author: debasishsing2020@gmail.com

studies based on LST is more popular due availability of more satellite sensor data like Landsat, MODIS and ASTER data [24-26]. Hence this current research attempted to focus on using the spatial pattern of UHI of Krishnanagar city of West Bengal by using four variable names LST, NDVI [27, 28], NDBI [29] and NDWI [30].

Using NDVI, we can monitor vegetation health and city climate studies. Built-up areas are susceptible to NDBI & NDWI is used to monitor the water content in vegetation. Also, built-up areas are subject to NDBI [31]. All the aforementioned techniques serve as useful proxy indicators for future urban planning.

Study Area

The study area includes Krishnanagar City and its surroundings in the Nadia district, which covers an area of approximately 273.19 square kilometer. The study area is located at 23° 22' 38" north latitude and 88°26'10" east longitude (Fig. 1). The average elevation of the study area is 17 meter above mean sea level. Nadia district is mostly cover with alluvial plains. Krishnanagar is classified as having a Tropical Savanna Climate (Köppen Climate Classification System, 1984), with a designation of "Aw." The mean annual temperature in the area is a little about 31°C, with peak temperatures in the summer that sporadically approach or surpass 34°C. Winter temperatures in Alipur, Kolkata, have risen over the last decade, resulting in shorter cold spells, according to the Indian Meteorological Department (IMD). The area receives an average yearly rainfall of around 1400 mm. The post-monsoon season, which lasts from September to November, follows the region's peak rainy season, which takes place in June and July. December through the middle of February is winter & March through May is summer, which means hot and muggy weather. Krishnanagar city and surrounding area is the most urbanised and populated place in Nadia. According to the 2011 Census, the total population of the city is 314,833, out of which 51% males and 49% females. Scheduled castes account for 35.96 percent of the population, while scheduled tribes account for 5.09 percent.

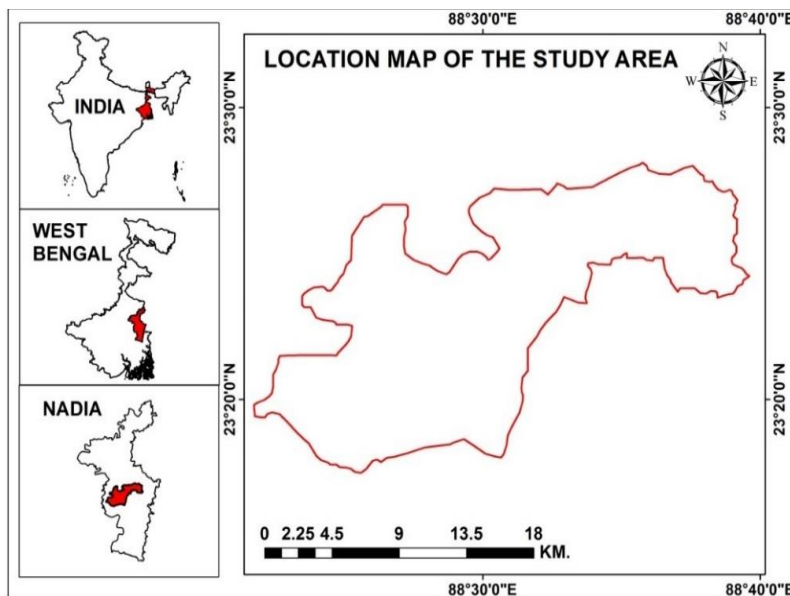


Fig. 1. Location map of Krishnanagar City

Methodology

Determination of emissivity

The surface temperature of terrain is controlled by the apparent emissions. We need NDVI threshold technique to find out the emissions, which is given by Sobrino, Jiménez-Munoz and Paolini as follows Equation (1):

$$NDVI = (\rho_{NIR} - \rho_{RED}) / (\rho_{NIR} + \rho_{RED}) \quad (1)$$

Land Surface Temperature retrieval

The land surface temperature (LST) modified for spectral emissivity was calculated by Carnahan and Artis (1982) as follows Equation (2),

$$LST = TB / \{ (1 + (\lambda \cdot TB / \rho) \cdot \ln \epsilon) \} \quad (2)$$

where: TB - satellite brightness temperature, λ - wavelength of emitted radiance in metre, ϵ - emissivity.

Conversion of spectral radiance to at-sensor brightness temperature Equation (3),

$$TB = \frac{K2}{\ln\left(\frac{K1}{L\lambda}\right) + 1} \quad (3)$$

Land use Land Cover Indices

The correlation between LST and LU/LC was determined using the NDVI, NDBI and NDWI indices [32, 33], which can be highly advantageous in monitoring and analysing the UHI of the study area. The following equations were used to obtain the LULC indices from satellite-based images:

$$NDVI = (NIR - R) / (NIR + R) \quad (4)$$

$$NDBI = (MIR - NIR) / (MIR + NIR) \quad (5)$$

$$NDWI = (G - MIR) / (G + MIR) \quad (6)$$

where the letters G, R, NIR and MIR stand in for the colours green, red, near infrared and mid-infrared, respectively.

Normalized Difference Vegetation Index:

By utilizing suitable bandcombinations, The NDVI is provided with pertinent vegetation feature information that helps differentiate between various vegetation features (Equation 4). Because vegetation responds spectrally to certain band combinations, it maximizes the quantity of vegetation data found in the total image.

IR stands for infrared light, and R stands for red light. NDVI = This calculation yields a number that ranges from -1 to +1. High reflectance in the NIR channel and low reflectance (or low values) in the red channel will result in a high NDVI rating, and vice versa. In actuality, it creates a consistent method of measuring healthy vegetation by utilizing the difference between these two bands. Healthy vegetation is seen in areas with high NDVI levels.

Normalized Difference Built up Index:

Normalized Difference Built up is a remote sensing index that uses satellite pictures to pinpoint populated and metropolitan regions. It makes use of the variation in reflectance values between the NIR and SWIR spectral bands, where populated regions often have lower reflectance in the NIR band and higher reflectance in the SWIR band. This indicator is useful for planning urban areas, keeping an eye on urban sprawl, and assessing how urbanization is affecting the environment. The range of the NDBI indices is -1 to 1 (Equation 5).

Normalized Difference Water Index:

A remote sensing technology called the Normalized Water Index (NWI) is used to detect and track water bodies in satellite pictures. Water bodies reflect more in the green band and

absorb more in the NIR band; therefore, it usually makes advantage of the difference in reflectance between these two spectral bands. The Normalized Difference Water indicator (NDWI) is one popular version of the indicator. An indicator called the Normalized Water indicator (NDWI) is used to identify water features in satellite photography (Equation 6). This index is helpful for monitoring changes in water bodies, managing water resources, and researching how drought and climate change affect water supply.

Linear Regression Analysis

We used multiple linear regressions to determine if LU/LC and LST were correlated. According to [34], it is the use of linear regression with multiple variables (Equation 7).

$$Y_i = \beta_0 + \beta_1 X_{i1} + \beta_2 X_{i2} + \dots + \beta_r X_{ir} + \epsilon_i \tag{7}$$

Several indices are used for mapping UHI for built-up area by many researchers [35, 36]. Regarding every pixel in the study area, we calculated the Urban Heat Island (UHI) and LULC index – NDBI, NDWI and NDVI [37]. Using GIS software (Arc-GIS), more than 3,000 random dots were extracted out of the LST image and their corresponding LULC index principles were identified. This information was then employed in the linear regression model to ascertain the association between LU/LC and LST [38, 39].

Results and discussion

Change of Land use/Land Cover in the Study Area

The algorithms involved in grouping or clustering of pixels to similar classes include unsupervised and supervised classification methods [40-43]. In the unsupervised method, as the name implies, algorithms are applied on the digital image to segregate pixels of similar DN values in all the selected bands with distance as the criterion. There are so many methods within the distance measurement such as Minimum distance, Euclidian distance and Cubical distance. Each method in its own way measure distance among pixels based on the intensity or DN values and classifies similar pixels into categories. For each of the three years, LULC maps were created and then area statistics were determined using the supervised maximum likelihood classification method shown in figure 2.

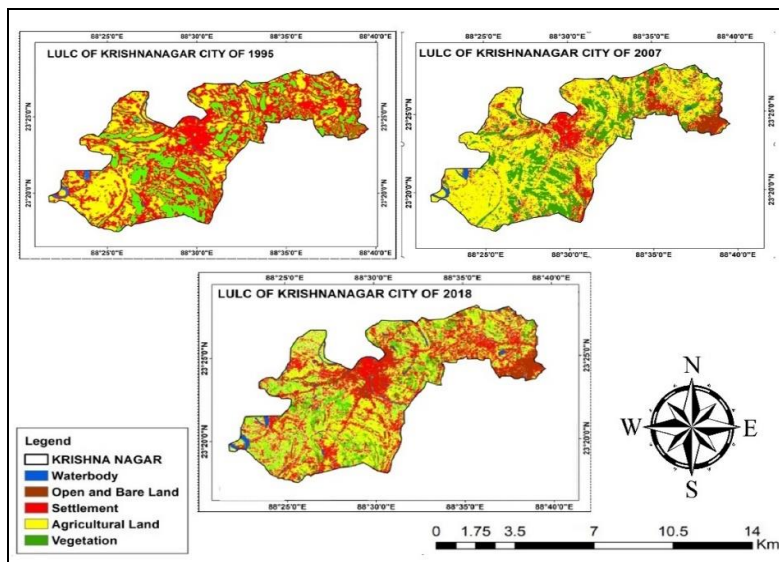


Fig. 2. LULC map of study area in 1995, 2007, 2018

Spatial pattern of Land Surface Temperature (LST)

The LST maps of the research region in 1995, 2007 and 2018 were obtained through data analysis [44]. Figure 3 shows that the LST varied from 24.54°C to 36.43°C in 1995, 24.54°C to 37.43°C in 2007 and 26.91°C to 37.84°C in 2018. The max. temperature increased by around 0.92°C in 1995 to 2007 and then also increased in the year 2018 by around 0.98°C. Between 1995 and 2007, the max. temperature enhanced by approximately 0.92°C and then again by around 0.98°C in 2018. In the subsequent years, meanwhile, the temperature progressively increases [45]. The Mean Land Surface Temperature in 1995, 2007, 2018 is shown in figure 4. Low temperature is shown by white tone in the middle of all maps, which represents the forest area, according to land surface temperature pattern analysis [46]. The impervious surface of the build-up and bare soil area is represented by a brown patch in the edges. The urban and agricultural area is represented by the centre yellow region. Due to the growing shift in land usage in this area, the land surface temperature is steadily rising [47].

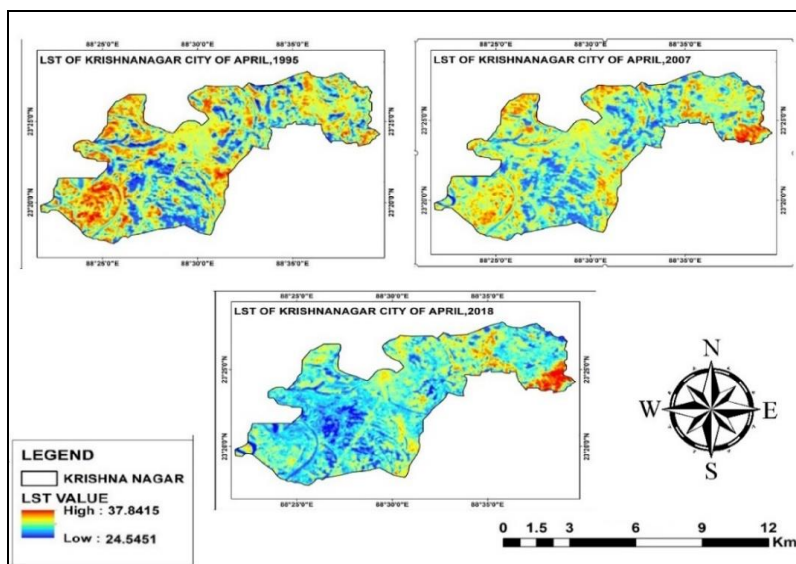


Fig. 3. LST map of the study area in 1995, 2007, 2018

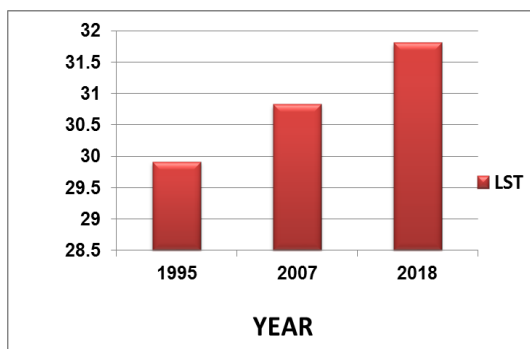


Fig. 4. Mean Land Surface Temperature in 1995, 2007, 2018

Normalized Difference Vegetation Index (NDVI)

As land surface temperature has a direct relation with vegetation cover, satellite derived vegetation index (NDVI) was also analysis for possible of UHI [48, 49]. The spatial distribution of NDVI values in the study area is represented in figure 5. It appeared that in the south-east

part of the city which represents the forest area has low NDVI values and southern part of the city observed highest NDVI value [50, 51].

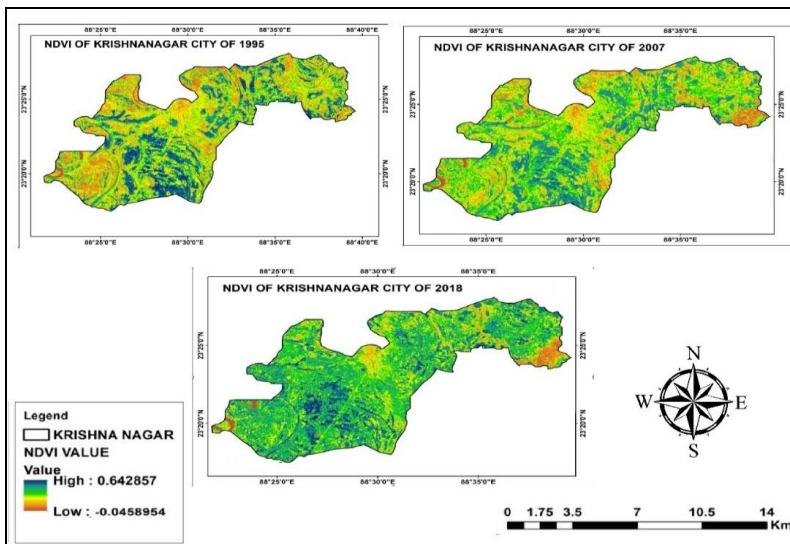


Fig. 5. Spatial design of Normalized Difference Vegetation Index in 1995, 2007, 2018

Normalized Difference Built-up Index (NDBI)

The NDBI technique is used for the extraction of built-up area using Thematic Mapper 5 satellite data (TM-5), which is accurate indicator of surface UHI effects was developed [52]. NDBI was the most positively correlated index for the urban land cover analysis. NDBI has a high spectral value in bare and urban areas (Fig. 6).

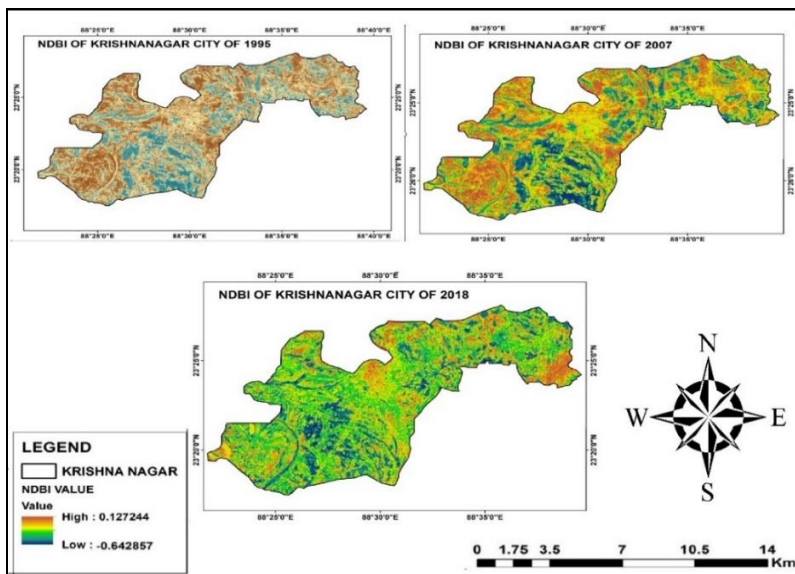


Fig. 6. Spatial model using NDBI in 1995, 2007, 2018

Urban areas have better reflectance in mid infrared (MIR) band of the electromagnetic spectrum resulting to higher NDBI value. The value of NDBI is increased due to the presence of dry vegetation in barren land and bare soil areas.

Normalized Difference Water Index (NDWI)

The water content of vegetation is estimated using the leaf area water-absent index, or the Normalised Difference Water Index (NDWI) [53, 54]. It measures the interaction of liquid water particles in vegetation with electromagnetic solar radiation. It is extensively used because, as compared to the NDVI, it is less sensitive to atmospheric scattering effects. The maximum NDWI value was found in the water content region and the lowest NDWI value was found in the barren soil land surface area, based on how NDWI is distributed spatially in the study region. The findings of this study show that from 1995 to 2007, the range of NDWI value somewhat decreases and then significantly decreases in 2018 (Fig. 7).

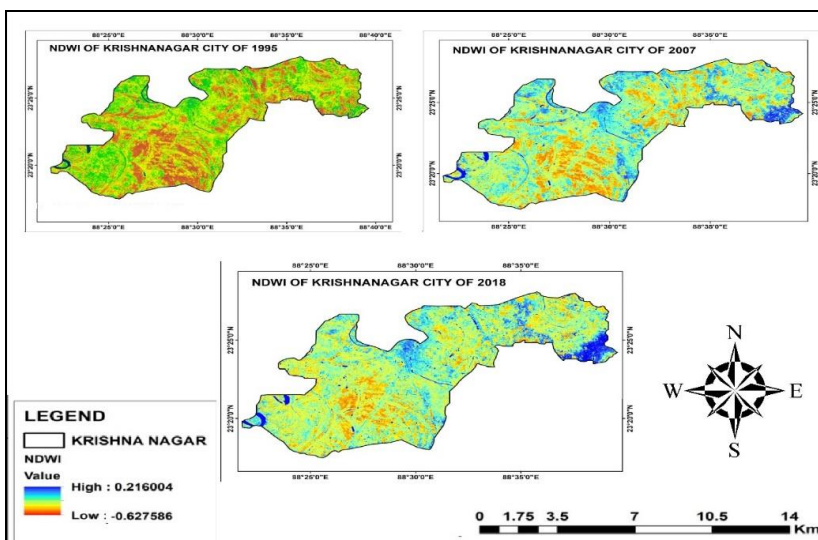


Fig. 7. Spatial model using NDWI in 1995, 2007, 2018

Effect of LST & LU/LC in Urban Heat Island

Linear Regression of LST and LU/LC indices

Linear regression method has commonly used for studying the correlation of LST with NDBI and NDVI [55]. In this research multiple linear regression was used to find out the relationship among LST, NDBI and NDVI which are independent variables to assess among the land surface temperature and land use and land cover (LU/LC) indices (Tables 1, 2, 3 and 4). After computing their correlation among NDVI, NDBI and NDWI, we discovered that there is a positive correlation between LST and NDBI, but a negative correlation between LST, NDWI and NDVI. The result shows that in the study area, the increase in built up area contributes to the increase in the LST. This illustrates the importance of vegetation in the mitigation of UHI effect.

Table 1. Shown highest, lowest and Mean Value of various Indices and LST

YEAR	NDVI			NDWI			NDBI			LST (0C)		
	High	Low	Mean	High	Low	Mean	High	Low	Mean	High	Low	Mean
1995	0.64	-0.28	-0.02	0.36	-0.62	-0.34	0.34	-0.64	0.01	36.43	24.54	29.91
2007	0.30	-0.25	-0.04	0.33	-0.44	-0.32	0.33	-0.30	0.04	37.43	24.54	30.83
2018	0.48	-0.04	0.26	0.21	-0.34	-0.12	0.12	-0.33	-0.11	37.84	26.91	31.81

Table 2. Indices showing correlation between LST and LULC in 2nd April, 1995

	LST	NDWI	NDBI	NDVI
LST	1.000	0.997	-0.998	-0.999
NDWI	0.997	1.000	-0.997	-0.998
NDBI	-0.998	-0.997	1.000	0.999
NDVI	-0.999	0.997	-0.998	1.000

Table 3. Indices showing correlation between LST and LULC in 4th April, 2007

	LST	NDWI	NDBI	NDVI
LST	1.000	.998	-1.000	-0.997
NDWI	0.998	1.000	-.998	-0.997
NDBI	-1.000	-0.998	1.000	0.996
NDVI	-0.997	-0.997	0.996	1.000

Table 4. Indices showing correlation between LULC and LST in 14th April, 2018

	LST	NDWI	NDBI	NDVI
LST	1.000	-0.932	0.976	-0.984
NDWI	-0.932	1.000	-0.858	0.942
NDBI	0.976	-0.858	1.000	-0.943
NDVI	-0.984	0.942	-0.943	1.000

A copious regression among LULC and the LST indices was done in 1995, 2007 and 2018, which is helpful in evaluating the thermal conductivity of the surroundings based on land use and land cover of the landscape. The regression models that were generated throughout the research are listed below (Figs. 8, 9 and 10). The unit of Land Surface Temperature is degree Centigrade.

$$\text{LST} = -5.440 \text{ NDVI} + 7.539 \text{ NDBI} - 2.316 \text{ NDWI} + 30.783 \quad (1995)$$

$$\text{LST} = -24.304 \text{ NDVI} - 15.499 \text{ NDBI} - 10.138 \text{ NDWI} + 30.086 \quad (2007)$$

$$\text{LST} = -12.309 \text{ NDVI} + 4.817 \text{ NDBI} + -5.275 \text{ NDWI} + 35.336 \quad (2018)$$

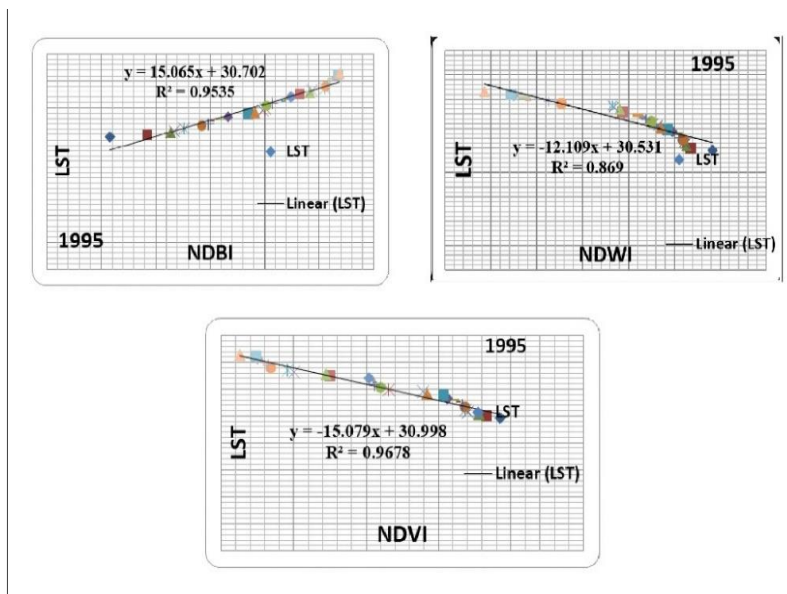


Fig. 8. Scatter Diagram Showing Correlations among LULC and LST indices in 1995

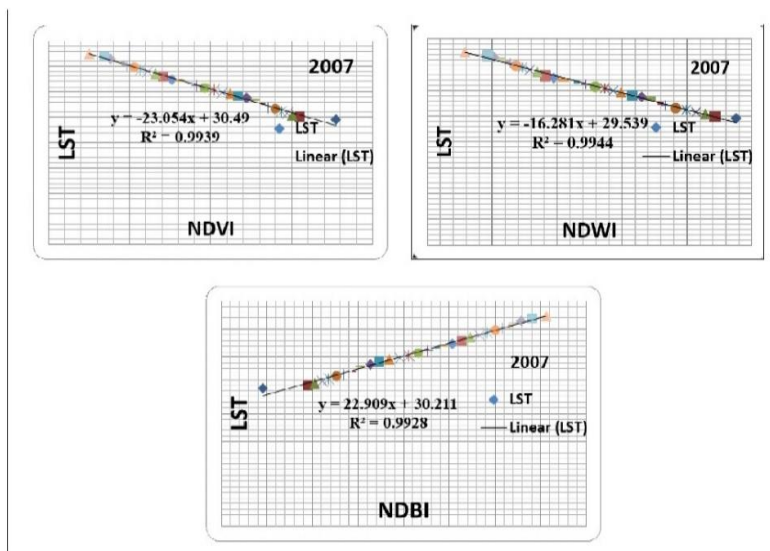


Fig. 9. Scatter Diagram Showing Correlations among LULC and LST indices in 2007

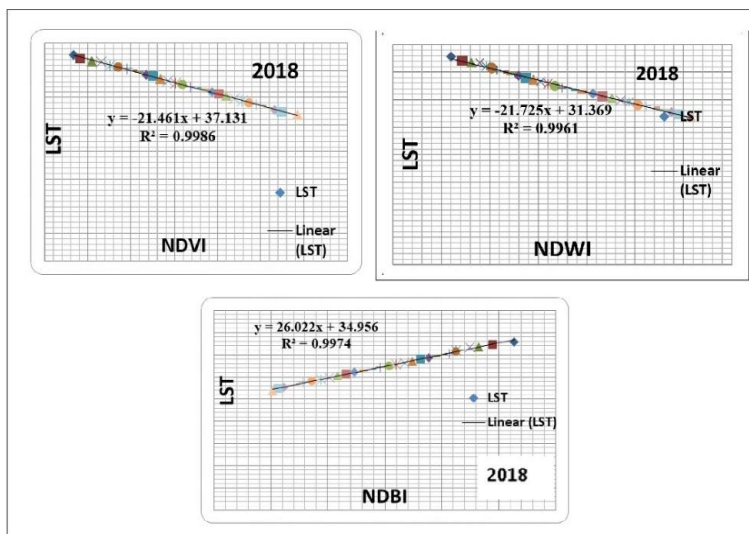


Fig. 10. Scatter Diagram Showing Correlations among LULC and LST indices in 2018

The Co-efficient, t-statistics, P-value, standard error and coefficient of determination (R^2) are all listed in Tables 5, 6, 7 respectively. The large value of the coefficient has a strong linear relationship of the regression model for all three years 1995, 2007 and 2018. In all cases, the value of “P” is close to zero, indicating that the indicators represent significant changes to the produced model. The coefficients of NDVI and NDWI have a large magnitude in 1995, indicating that they have a significant influence on LST. In 2007, the value of the NDWI, NDBI and NDVI are about equal. However, in 2018, the value of NDVI and NDWI is significantly more than that of value of NDBI.

Table 5. Regression Analysis Parameters in 2nd April, 1995

	Approximate	Standard error	t- Value	P Value	R ²
Constant	30.783	0.068	450.505	0.00	
NDWI	-2.316	0.683	-3.392	0.00	
NDBI	7.539	0.817	9.226	0.00	0.993
NDVI	-5.440	1.243	-4.376	0.00	

Table 6. Regression Analysis Parameters in 4th April, 2007

	Approximate	Standard error	t- Value	P Value	R ²
Constant	30.086	.260	30.086	0.00	
NDWI	-10.138	3.845	-10.138	0.00	
NDBI	-15.499	13.126	-15.499	0.00	0.995
NDVI	-24.304	13.469	-24.304	0.00	

Table 7. Regression Analysis Parameters in 14th April, 2018

	Estimate	Standard error	t- Value	P-Value	R ²
Constant	35.336	.383	92.169	0.00	
NDWI	-5.275	1.593	-3.311	0.00	
NDBI	4.817	2.615	1.842	0.00	0.999
NDVI	-12.309	2.051	-6.001	0.00	

Hotspot Analysis for Land Surface Temperature (LST)

According to the hotspot analysis the drastic changes of LST observe from 1995 to 2007 and it is slightly decreased in the year 2018 which shown in figure 11.

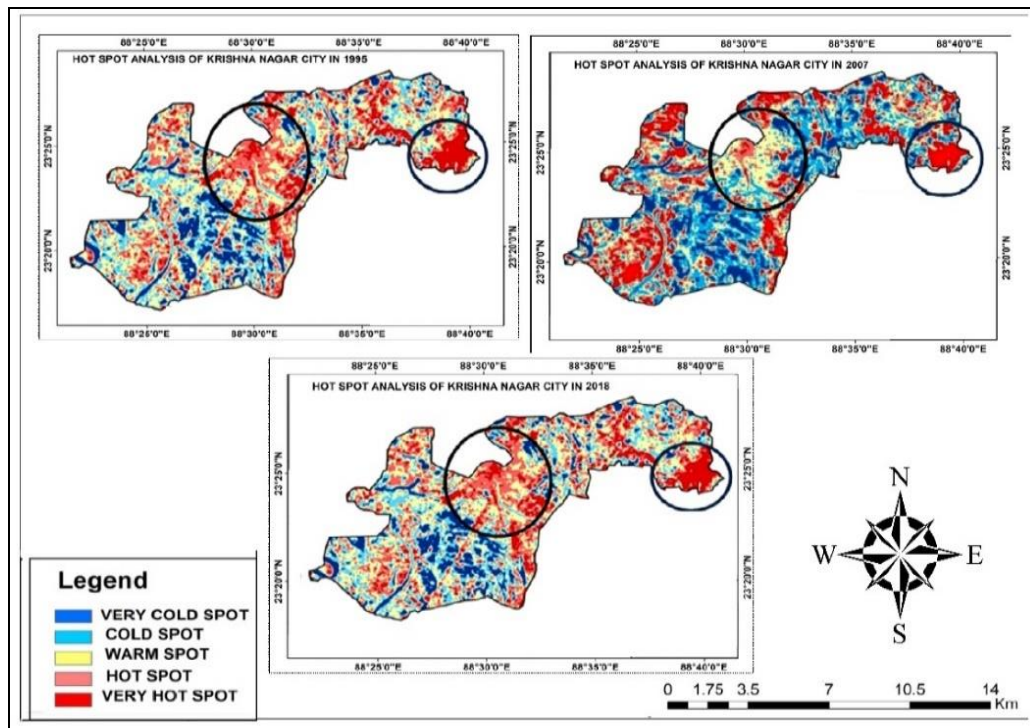


Fig. 11. Spatial pattern of Hot Spot in the Krishnagar city in 1995, 2007, 2018

In the years 2007 and 2018, a large heat island formed that covered almost the whole central urban area, as well as barren soil and the surrounding area. This heat island is shown in the east part of the study area. On the other hand, from 2007 to 2018, the cold zone in the Krishnanagar area's west and south-west has gradually disappeared [56-58].

Conclusions

The findings of this study reveal an increase in UHI impacts in the research area between 1995 and 2018 and numerous differences could be detected. Low LST value were found in the green regions, especially in the southwestern section of the research area, whereas high LST clusters were detected in built-up and densely populated areas. The formation of UHI in the study area is owing to a loss in vegetation cover as well as the increase of built-up areas. As a result, vegetation cover is a critical feature in preventing direct solar radiation exposure of the ground surface. Through evaporation, an increase in vegetation cover aids in the creation of a cool island effect.

As a result, future landscape and urban reforestation, particularly in Krishnanagar UHI hot spot region, is necessary. Parkland, tree cover and vegetation cover should be increased in different location like in school, hospital, temple, Government office to minimize UHI effect.

The findings of this study may aid in better understanding of the emergence of UHI in Krishnanagar city and its surroundings. Urban planners and policymakers should pay more attention to preventing or controlling the emergence of UHI in these urban areas. In the future, new green urban development is expected to be developed in Krishnanagar, West Bengal, to reduce adverse UHI consequences, according to this study.

Acknowledgments

The authors are grateful to the CNPq National Council of Scientific and Technologic Development for supporting this project, to the Center for Lasers and Applications' Multiuser Facility at IPEN-CNEN/SP and to Anton Paar Brasil for the use of the Raman spectrometer. We also thank Teodora Camargo and Tatiana Russo from the *Núcleo de Conservação e Restauro in Pinacoteca do Estado de São Paulo* for their invaluable contributions.

References

- [1] P.H. Verburg, N. Crossman, E.C. Ellis, A. Heinimann, P. Hostert, O. Mertz, H. Nagendra, T. Sikor, K. Erb, N. Golubiewski, R. Grau, M. Grove, S. Konaté, P. Meyfroidt, D.C. Parker, R.R. Chowdhury, H. Shibata, A. Thomson, L. Zhen, *Land system science and sustainable development of the earth system: A global land project perspective*, **Anthropocene**, **12**, 2015, pp. 29-41. <https://doi.org/10.1016/j.ancene.2015.09.004>.
- [2] B. Rotich, D. Ojwang, D. (2021). *Trends and drivers of forest cover change in the Cherangany hills forest ecosystem, western Kenya*, **Global Ecology and Conservation**, **30**, 2021, Article Number: e01755. DOI: 10.1016/j.gecco.2021.e01755.
- [3] L.S. Miles, S.T. Breitbart, H.H. Wagner, M.T. Johnson, *Urbanization shapes the ecology and evolution of plant-arthropod herbivore interactions*, **Frontiers in Ecology and Evolution**, **7**, 2019, Article Number: 310. DOI: 10.3389/fevo.2019.00310.

- [4] G. Fage Ibrahim, (2017). *Urban land use land cover changes and their effect on land surface temperature: Case study using Dohuk city in the Kurdistan region of Iraq*, **Climate**, **5**(1), 2017, Article Number: 13. DOI:10.3390/cli5010013.
- [5] S. Kato, Y. Yamaguchi, *Analysis of urban heat-island effect using ASTER and ETM+ data: Separation of anthropogenic heat discharge and natural heat radiation from sensible heat flux*, **Remote Sensing of Environment**, **99**(1-2), 2005, pp. 44-54. DOI: 10.1016/j.rse.2005.04.026.
- [6] L.V. Anh, T.A. Tuan, *Estimation of land surface temperature using emissivity calculated from normalized difference vegetation index*, **Vietnam Journal of Earth Sciences**, **36**(2). 2014, pp. 184–192. DOI:10.15625/0866-7187/36/2/450.
- [7] K.P. Gallo, T.W. Owen, *Assessment of urban heat islands: A multi-sensor perspective for the Dallas-FT. worth, USA region*, **Geocarto International**, **13**(4), 1998, pp. 35-41. DOI:10.1080/10106049809354662.
- [8] C. Johnson, *Green networks: A solution to the urban heat island effect*, **Sustainable Development and Planning 2024, (The Sustainable City X)** **195**, 2015, pp. 205-214. DOI: 10.2495/sc150191.
- [9] X. Zhang, R.C. Estoque, Y. Murayama, M. Ranagalage, *Capturing urban heat island formation in a subtropical city of China based on Landsat images: Implications for sustainable urban development*, **Environmental Monitoring and Assessment**, **193**(3) 2021, Article Number: 130. DOI:10.1007/s10661-021-08890-w.
- [10] B. Khorrami, O. Gunduz, *Spatio-temporal interactions of surface urban heat island and its spectral indicators: A case study from Istanbul metropolitan area, Turkey*, **Environmental Monitoring and Assessment**, **192**(6), 2020, DOI: 10.1007/s10661-020-08322-1.
- [11] M. Gao, H. Shen, X. Han, H. Li, L. Zhang, *Multiple timescale analysis of the urban heat island effect based on the community land model: A case study of the city of Xi'an, China*, **Environmental Monitoring and Assessment**, **190**(1), 2017, Article Number: 8. DOI: 10.1007/s10661-017-6320-9.
- [12] AZAHRA, A. F., NURJANI, E., & SEKARANOM, A. B. (2024). The influence of land cover on spatio-temporal variation of air temperature in Grogol district, Central Java – Indonesia. *International Journal of Conservation Science*, *15*(1), 1021-1032. <https://doi.org/10.36868/ijcs.2024.02.18>
- [13] S.N. Goward, *Thermal Behavior of Urban Landscapes and the Urban Heat Island*, **Physical Geography**, **2**(1), 1981, pp. 19-33.
- [14] S. Barad, P. Mishra, P.C. Sahu, T. Sarkar, M.F. Amin, T. Choudhury, H.A. Edinur, Z.A. Kari, D. Nandi, S. Pati, *Comparative approach of decision tree and CWQI analysis for classification of groundwater with a special reference to fluoride ion in drought-prone Boudh district of Odisha, India*, **Sustainable Water Resources Management**, **7**(6). Article Number: 94. DOI: 10.1007/s40899-021-00582-0.
- [15] S. Pati, S. Shahimi, D. Nandi, T. Sarkar, S. Acharya, H. Sheikh, D.K. Acharya, T. Choudhury, Akbar John, B.R. Nelson, B.P. Dash, H. Edinur, *Predicting Tachypleusgigas spawning distribution with climate change in Northeast coast of India*, **Journal of Ecological Engineering**, **22**(3), 2021, pp. 211-220. DOI: 10.12911/22998993/131244.
- [16] P. Mishra, D. Nandi, P. Sahu, K. Mohanta, H. Edinur, T. Sarkar, S. Pati, *Hydro-geochemical attributes-based classifiers for groundwater analysis*, **Ecological**

- Engineering & Environmental Technology**, **22**(5), 2021, pp. 28-39. DOI: 10.12912/27197050/139412.
- [17] B. Rimal, *Urban Growth and Land use/Land cover change of PokharaSubMetropolitan city, Nepal*, **Journal of Theoretical and Applied Information Technology**, **26**(2), 2011, pp. 118-129.
- [18] D. Nandi, S. Mishra, *Groundwater quality mapping by using geographic information system (gis): a case study of Baripada city, Odisha India*, **International Journal of Conservation Science**, **5**(1), 2014, pp. 79–84.
- [19] D.E. Parker, *Urban heat island effects on estimates of observed climate change*, **Wiley Interdisciplinary Reviews: Climate Change**, **1**(1), 3010, pp. 123–133.
- [20] V. Mishra, A.R. Ganguly, B. Nijssen, D.P. Lettenmaier, *Changes in observed climate extremes in global urban areas*, **Environmental Research Letters**, **10**(2), 2015, Article Number: 024005. DOI: 10.1088/1748-9326/10/2/024005.
- [21] J. Tan, Y. Zheng, X. Tang, C. Guo, L. Li, G. Song, X. Zhen, D. Yuan, A.J. Kalkstein, F. Li, *The urban heat island and its impact on heat waves and human health in Shanghai*, **International Journal of Biometeorology**, **54**(1), 2010, pp. 75-84. DOI: 10.1007/s00484-009-0256-x.
- [22] M.W. Yahia, E. Johansson, S. Thorsson, F. Lindberg, M.I. Rasmussen, *Effect of urban design on microclimate and thermal comfort outdoors in warm-humid Dar es Salaam, Tanzania*, **International Journal of Biometeorology**, **62**(3), 2017, pp. 373-385. DOI:10.1007/s00484-017-1380-7.
- [23] J.P. Kim, J.M. Guldman, *Land-Use Planning and the Urban Heat Island*, **Environmental and Planning B: Planning and Design**, **41**(6), 2014, pp. 1077-1099. DOI: 10.1068/b130091p.
- [24] M.L. Imhoff, P. Zhang, R.E. Wolfe, L. Bounoua, *Remote sensing of the urban heat island effect across biomes in the continental USA*, **Remote Sensing of Environment**, **114**(3), 2010, pp. 504-513. DOI: 10.1016/j.rse.2009.10.008.
- [25] Y. Zeng, H. Li, B. Xue, H. Zhang, *Assessment of surface urban heat island effects and associated surface biophysical indicators using MODIS imagery*, **Geoinformatics 2007: Remotely Sensed Data and Information**, **6752**(1-2), 2007, Article Number: 67521S. DOI:10.1117/12.760708.
- [26] J.A. Sobrino, J.C. Jiménez-Muñoz, L. Paolini, L. (2004). *Land surface temperature retrieval from LANDSAT TM 5*, **Remote Sensing of Environment**, **90**(4), 200, pp. 434-440. DOI: 10.1016/j.rse.2004.02.003.
- [27] J.W. Rouse, R.H. Haas, J.A. Schell, D.W. Deering, *Monitoring Vegetation Systems in the GreatPlains with ERTS*, **Proceedings of the Third ERTS Symposium NASA SP-351**, Washington, DC, USA, 10–14; Vol. 1, 1974, pp. 309–317.
- [28] J. Goswami, S. Roy, S. Sudhakar, *A Novel Approach in Identification of Urban Hot Spot Using Geospatial Technology: A Case Study in Kamrup Metro District of Assam*, **International Journal of Geosciences**, **4**(5), 2013, pp. 898-903. DOI: 10.4236/ijg.2013.45084.
- [29] Y. Zha, J. Gao, S. Ni, *Use of normalized difference built-up index in automatically mapping urban areas from TM imagery*, **International Journal of Remote Sensing**, **24**, 2005, pp. 583–594. DOI: 10.1080/01431160304987.

- [30] B.C. Gao, *NDWI—A normalized difference water index for remote sensing of vegetation liquid water from space*, **Remote Sensing of Environment**, **58**(3), 1996, pp. 257–266. DOI: 10.1016/S0034-4257(96)00067-3.
- [31] X.L. Chen, H.M. Zhao, P.X. Li, Z.Y. Yin, *Remote sensing image-based analysis of the relationship between urban heat island and land use/cover changes*, **Remote Sensing of Environment**, **104**(2), 2006, pp. 133–146, Special Issue 1. DOI: 10.1016/j.rse.2005.11.016.
- [32] O. Orhan, S. Ekercin, F. Dadaser-Celik, *Use of Landsat land surface temperature and vegetation indices for monitoring drought in the Salt Lake basin area, Turkey*, **Scientific World Journal**, **2014**, 2014, Article Number: 142939. DOI: 10.1155/2014/142939.
- [33] A.-A. Kafy, N.N. Dey, A. Al Rakib, Z.A. Rahaman, N.M.R. Nasher, A. Bhatt, *Modeling the relationship between land use/land cover and land surface temperature in Dhaka, Bangladesh using CA-ANN algorithm*, **Environmental Challenges**, **4**, 2021, Article Number: 100190. DOI: 10.1016/j.envc.2021.100190.
- [34] D. Choudhury, K. Das, A. Das, *Assessment of land use land cover changes and its impact on variations of land surface temperature in Asansol-durgapur development region*, **The Egyptian Journal of Remote Sensing and Space Science**, **22**(2), 2019, pp. 203–218. DOI: 10.1016/j.ejrs.2018.05.004
- [35] J. Higgins, **The Radical Statistician**, 2005, Last visit, 1/10/2017, [http:// www. biddle. Om/ documents/ bcg_comp_chapter4.pdf](http://www.biddle.Om/documents/bcg_comp_chapter4.pdf).
- [36] C. He, P. Shi, D. Xie, Y. Zhao, *Improving the normalized difference built-up index to map urban built-up areas using a semiautomatic segmentation approach*, **Remote Sensing Letters**, **1**, 2010, pp. 213–221.
- [37] M. Kawamura, S. Jayamana, Y. Tsujiko, *Relation between Social and Environmental Conditions in Colombo Sri Lanka and the Urban Index Estimated by Satellite Remote Sensing Data. Int. Arch., Photogrammetry. Remot Sensing*, **31**, 1996, pp. 321–326.
- [38] Q. Weng, D. Lu, J. Schubring, *Estimation of land surface temperature–vegetation abundance relationship for urban heat island studies*, **Remote Sensing of Environment**, **89**(4), 2004, pp. 467–483. DOI: 10.1016/j.rse.2003.11.005.
- [39] Y. Zhang, I.O. Odeh, C. Han, *Bi-temporal characterization of land surface temperature in relation to impervious surface area, NDVI and NDBI, using a sub-pixel image analysis*, **International Journal of Applied Earth Observation and Geoinformation**, **11**(4), 2009, pp. 256–264. DOI: 10.1016/j.jag. 2009.03.001.
- [40] F. Yuan, M.E. Bauer, *Comparison of impervious surface area and normalized difference vegetation index as indicators of surface urban heat island effects in Landsat imagery*, **Remote Sensing of Environment**, **106**(3), 2007, pp. 375–386. DOI: 10.1016/j.rse.2006.09.003.
- [41] M.K. Leta, T.A. Demissie, J. Tränckner, *Modeling and prediction of land use land cover change dynamics based on land change modeler (LCM) in Nashe watershed, upper Blue Nile basin, Ethiopia*, **Sustainability**, **13**(7), 2021, Article Number: 3740. DOI:10.3390/su13073740.
- [42] G. Sisay, G. Gitima, M. Mersha, W.G. Alemu, *Assessment of land use land cover dynamics and its drivers in Bechet watershed upper Blue Nile basin, Ethiopia*, **Remote Sensing Applications: Society and Environment**, **24**, 2021, Article Number: 100648. DOI: 10.1016/j.rsase.2021.100648.

- [43] J.P. Koshale, C. Singh, *Multi-temporal land use/Land cover (LULC) change analysis using remote sensing and GIS techniques of Durg block, Durg district, Chhattisgarh, India, Sustainable Development Practices Using Geoinformatics*, 2020, pp. 185-204. DOI: 10.1002/9781119687160.ch12.
- [44] M.S. Cho, J. Qi, *Quantifying spatiotemporal impacts of hydro-dams on land use/land cover changes in the lower Mekong River basin, Applied Geography*, **136**, 2021, Article Number: 102588. DOI: 10.1016/j.apgeog.2021.102588.
- [45] J. Li, C. Song, L. Cao, F. Zhu, X. Meng, J. Wu, *Impacts of landscape structure on surface urban heat islands: A case study of Shanghai, China, Remote Sensing of Environment*, **115**(12), 2011, pp. 3249-3263. DOI: 10.1016/j.rse.2011.07.008.
- [46] S. Guha, H. Govil, *An assessment on the relationship between land surface temperature and normalized difference vegetation index, Environment, Development and Sustainability*, **23**(2), 2020, pp. 1944-1963. DOI:10.1007/s10668-020-00657-6.
- [47] Q. Weng, *A remote sensing–GIS evaluation of urban expansion and its impact on surface temperature in the Zhujiang delta, China, International Journal of Remote Sensing*, **22**(10), 2001, pp. 1999-2014. DOI:10.1080/01431160118847.
- [48] J. Tan, R. Belcher, H. Tan, S. Menz, T. Schroepfer, *The urban heat island mitigation potential of vegetation depends on local surface type and shade, Urban Forestry & Urban Greening*, **62**, 2021, Article Number: 127128. DOI: 10.1016/j.ufug.2021.127128.
- [49] H. Govil, S. Guha, P. Diwan, N. Gill, A. Dey, *Analyzing linear relationships of LST with NDVI and MNDISI using various resolution levels of Landsat 8 OLI and TIRS data, Data Management, Analytics and Innovation*, 2019, pp. 171-184. DOI:10.1007/978-981-32-9949-8_13.
- [50] A. Sekertekin, E. Zadbagher, *Simulation of future land surface temperature distribution and evaluating surface urban heat island based on impervious surface area, Ecological Indicators*, **122**, 2021, Article Number: 107230. DOI: 10.1016/j.ecolind.2020.107230
- [51] A. Sekertekin, S. Bonafoni, *Land surface temperature retrieval from Landsat 5, 7, and 8 over rural areas: Assessment of different retrieval algorithms and emissivity models and toolbox implementation, Remote Sensing*, **12**(2), 2020, Article Number: 294. DOI:10.3390/rs12020294.
- [52] J.A. Gamon, C.B. Field, M.L. Goulden, K.L. Griffin, A.E. Hartley, G. Joel, J. Peñuelas, R. Valentini, *Relationships between NDVI, canopy structure, and photosynthesis in three californian vegetation types, Ecological Applications*, **5**(1), 1995, pp. 28-41. DOI: 10.2307/1942049.
- [53] N.R. Wilson, L.M. Norman, M. Villarreal, L. Gass, R. Tiller, A. Salywon, *Comparison of remote sensing indices for monitoring of desert cienegas, Arid Land Research and Management*, **30**(4), 2016, pp. 460-478. DOI:10.1080/153.24982.2016.1170076.
- [54] S.K. McFeeters, *The use of the Normalized Difference Water Index (NDWI) in the delineation of open water features, International Journal of Remote Sensing*, **17**, 1996, pp. 1425–1432.
- [55] T. Jackson, *Vegetation water content mapping using Landsat data derived normalized difference water index for corn and soybeans, Remote Sensing of Environment*, **92**(4), 2004, pp. 475-482. doi: 10.1016/j.rse.2003.10.021.
- [56] G.L. Feyisa, H. Meilby, G.D. Jenerette, S. Pauliet, *Locally optimized separability enhancement indices for urban land cover mapping: Exploring thermal environmental*

consequences of rapid urbanization in Addis Ababa, Ethiopia, **Remote Sensing of Environment**, **175**, 2016, pp. 14–31.

- [57] A.M. Coutts, E.C. White, N.J. Tapper, J. Beringer, S.J. Livesley, S. J. (2015). *Temperature and human thermal comfort effects of street trees across three contrasting street canyon environments*, **Theoretical and Applied Climatology**, **124**(1-2), 2015, pp. 55-68. DOI: 10.1007/s00704-015-1409-y
- [58] J.M. Rodriguez Lopez, K. Heider, J. Scheffran, *Frontiers of urbanization: Identifying and explaining urbanization hot spots in the south of Mexico City using human and remote sensing*, **Applied Geography**, **79**, 2017, pp. 1-10. DOI: 10.1016/j. apgeog. 2016.12.001

Received: July 22, 2023

Accepted: August 21, 2024